Received: 14 June 2017 | Revised: 30 August 2017 | Accepted: 31 August 2017

DOI: 10.1111/pce.13071

WILEY Plant, Cell & Environment

ORIGINAL ARTICLE

In situ temperature relationships of biochemical and stomatal controls of photosynthesis in four lowland tropical tree species

Martijn Slot | Klaus Winter

Smithsonian Tropical Research Institute, Apartado 0843-03092, Balboa, Ancón, Republic of Panama

Correspondence
Martijn Slot, Smithsonian Tropical Research Institute, Apartado 0843-03092, Balboa, Ancón, Republic of Panama.
Email: martijnslot78@gmail.com

Abstract

Net photosynthetic carbon uptake of Panamanian lowland tropical forest species is typically optimal at 30–32 °C. The processes responsible for the decrease in photosynthesis at higher temperatures are not fully understood for tropical trees. We determined temperature responses of maximum rates of RuBP-carboxylation (V_{CMax}) and RuBP-regeneration (J_{Max}), stomatal conductance (G_s), and respiration in the light (R_{Light}) in situ for 4 lowland tropical tree species in Panama. G_s had the lowest temperature optimum (T_{Opt}), similar to that of net photosynthesis, and photosynthesis became increasingly limited by stomatal conductance as temperature increased. J_{Max} peaked at 34–37 °C and V_{CMax} ~2 °C above that, except in the late-successional species *Calophyllum longifolium*, in which both peaked at ~33 °C. R_{Light} significantly increased with increasing temperature, but simulations with a photosynthesis model indicated that this had only a small effect on net photosynthesis. We found no evidence for Rubisco-activase limitation of photosynthesis. T_{Opt} of V_{CMax} and J_{Max} fell within the observed in situ leaf temperature range, but our study nonetheless suggests that net photosynthesis of tropical trees is more strongly influenced by the indirect effects of high temperature—for example, through elevated vapour pressure deficit and resulting decreases in stomatal conductance—than by direct temperature effects on photosynthetic biochemistry and respiration.

KEYWORDS

climate change, global warming, J_{Max}, photosynthetic temperature responseplant functional types, R_{Light}, stomatal conductancetropical forest, V_{CMax}, VPD

1 | INTRODUCTION

Because of the importance of tropical forests to the global carbon cycle (Pan et al., 2011; Pan, Birdsey, Phillips, & Jackson, 2013; Schimel, Stephens, & Fisher, 2015), there is a need to improve their representation in Earth system models (e.g., Norby et al., 2017). More specifically, a better understanding is needed of the effects of temperature on the carbon exchange properties of tropical forest trees. A recent survey showed that the temperature optimum for net photosynthesis (T_{Opt}) converged on mean daytime temperatures across 42 tropical tree and liana species in Panama (Slot & Winter, 2017a), consistent with observations of stand-level photosynthesis across tropical sites (Tan et al., 2017). Observations of decreasing net carbon uptake above current ambient temperatures raise questions about how close to a high-temperature threshold tropical forests operate (Doughty & Goulden, 2008). Above T_{Opt}, both stomatal and biochemical factors become increasingly limiting to net photosynthesis (Sage & Kubien, 2007), but biochemical parameters were not rigorously assessed in the survey of Slot and Winter (2017a). Such an assessment, together with information on stomatal conductance will be essential to identify the mechanisms determining the temperature-responses of net carbon uptake by tropical forest trees.

The temperature response of photosynthesis of fully illuminated leaves is controlled by photosynthetic biochemistry, stomatal conductance, and the rate of respiration in the light (Lin, Medlyn, & Ellsworth, 2012). At current ambient atmospheric [CO_2], the dominant biochemical limitation at suboptimal temperatures is triose phosphate utilization (TPU), a limitation of inorganic phosphate for photophosphorylation caused by low rates of starch and sucrose synthesis (Sage & Kubien, 2007). At higher temperatures, the maximum rate of RuBP-carboxylation (V_{CMax}) and the maximum rate of RuBP-regeneration (J_{Max})—generally assumed to reflect photosynthetic electron transport—become limiting, with deactivation of Rubisco caused by heat-sensitive Rubisco activase probably also playing a role at supra-optimal temperatures (Crafts-Brandner & Salvucci, 2000; Sage

& Kubien, 2007). V_{CMax} and J_{Max} are commonly assumed to either increase in an exponential fashion with increasing temperature or to show a peaked temperature response (Medlyn et al., 2002). Stomatal conductance (G_s) has a peaked temperature response, which reflects the balance between a positive direct effect of temperature on stomatal opening, and a negative indirect effect, as leaf-to-air vapour pressure deficit (VPD) increases with increasing temperature causing G_s to decrease (Peak & Mott, 2011). Non-photorespiratory mitochondrial respiration in the light (R_{Light}) increases near-exponentially with temperature over ecologically relevant temperature ranges (Way, Oren, & Kroner, 2015) and may significantly lower net photosynthesis rates at high temperature (Way & Yamori, 2014). Although reasonably well understood conceptually, these temperature-response parameters are not sufficiently quantified for tropical forest species, and the temperature response of tropical vegetation remains a key uncertainty in terrestrial carbon modelling (e.g., Ahlström, Schurgers, Arneth, & Smith, 2012; Cox et al., 2013; Huntingford et al., 2013; Rowland et al., 2015).

To improve the representation of tropical forests in Earth system models, the relationships of V_{CMax} and J_{Max} with leaf nutrients have recently been determined for a large number of tropical forest species (Bahar et al., 2017; Norby et al., 2017). Bahar et al. (2017) reported that V_{CMax} and J_{Max} at 25 °C decreased with increasing mean annual temperature along an elevation gradient, but local temperature responses were not determined at any site. Lack of such data may have consequences for model performance. For example, Rowland et al. (2015) found that when simulating photosynthesis in tropical forests, the uncertainty in, and the difference across, sophisticated vegetation models increased with temperature, in part because the models used different temperature optima for V_{CMax}. T_{Opt} values ranged from 30 °C in the SPA model (Williams, 1996) to 41 °C in ED2 (Medvigy, Wofsy, Munger, Hollinger, & Moorcroft, 2009), and V_{CMax} at T_{Opt} varied by >50% across the models. Variation in estimates of V_{CMax} (and J_{Max}) at a set temperature can be reduced by determining their relationship with foliar nutrient content (Bahar et al., 2017; Norby et al., 2017), but empirical data on temperature responses of V_{CMax} and J_{Max} will be critical to constrain the temperature relationships and improve the representation of photosynthesis in Earth system models (Rogers et al., 2017).

We measured V_{CMax}, J_{Max}, G_s, and R_{Light} on free-growing saplings and trees of four ecologically contrasting lowland tropical tree species across a range of leaf temperatures to determine the temperature optima and temperature-sensitivities of these parameters and to evaluate species differences. In addition, we determined whether the temperature sensitivity of Rubisco activase influenced photosynthetic performance over ecologically relevant temperature ranges. Photorespiration (R_p), the oxygenation of Rubisco that leads to a loss of CO_2, represents another biochemical limitation of net carbon gain that increases with rising temperature (Brooks & Farquhar, 1985), but this was not studied, as the available non-destructive methods for estimating R_p require accurate assessment of mesophyll conductance currently not available for our target species. Based on previous measurements of the temperature response of tree and liana net photosynthesis (Slot & Winter, 2017a) and dark respiration (Slot, Rey-Sánchez, Winter, & Kitajima, 2014; Slot, Wright, & Kitajima, 2013) in Panama, we hypothesized that the process rates would be higher in early successional species than in late-successional species, but that the thermal optima and the rate of increase in R_{Light} with measurement temperature would be similar across species. To avoid the risk of measurement artefacts caused by excising branches (Santiago & Mulkey, 2003) or by artificial growth conditions, all measurements were made on attached leaves in situ.

2 | MATERIALS AND METHODS

2.1 | Plant material

Four common tree species, with one or more field-grown individuals with accessible leaves, were selected at the Santa Cruz Experimental Field Facility of the Smithsonian Tropical Research Institute in Gamboa, Panama (Table 1).Two of these were early successional species and two were late-successional, enabling us to evaluate potential differences between plant functional types. The late-successional trees grew on the forest edge, receiving full solar radiation from mid-morning till mid-afternoon; the early successional species were more permanently sun exposed. Soils at the site are classified as Alfisols. Mean annual temperature is 26.9 °C, with mean daily minima and maxima of 23.7 and 32.6 °C, respectively. Annual rainfall averages 2,058 mm, >80% of which falls between May and December (data from 2014 to 2016, meteorological data collected on site). *Ficus insipida* Willd. is an early successional species that is most common in young or disturbed forests; *Lagerstroemia speciosa* (L.) Pers. is an introduced ornamental tree that is associated with open habitats and secondary forest in its native range in south Asia; *Calophyllum longifolium* Willd. is a late-successional species that is widespread in mature forests; and *Garcinia madruno* (Kunth) Hammel is a late-successional species associated with wet forests. The three native species are all broadly distributed throughout tropical South and Central America. All trees were planted, the *L. speciosa* trees ~25 years ago, the others in early 2014, when they were about 1 year old.

TABLE 1 Tree species studied and their characteristics, including whether or not they are latex-producing; the number and estimated mean height ($\widehat{h}$) and age of the individuals; the number of A-C_i curves included in the final analyses, and the temperature range (T_{Leaf} range) over which they were measured

Functional group	Species	Family	Latex	Trees	$\widehat{h}$ (m)	$\widehat{Age}$ (y)	Curves	T_{Leaf} range (°C)	LMA (gm^{-2})	N (%)
Early successional	*Ficus insipida* Willd.	Moraceae	Y	1	7	4	34	26.8–38.4	109 ± 7	2.5 ± 0.3
	Lagerstroemia speciosa (L.) Pers.	Lythraceae	N	2	8	25	47	27.9–40.8	87 ± 9	2.4 ± 0.1
Late successional	*Calophyllum longifolium* Willd.	Clusiaceae	Y	2	5	4	28	27.9–37.8	175 ± 4	1.0 ± 0.0
	Garcinia madruno (Kunth) Hammel	Clusiaceae	Y	3	3	4	40	29.6–38.5	136 ± 10	1.1 ± 0.1

Note. Leaf mass per unit leaf area (LMA) and leaf nitrogen (N) content (±SD) were determined for three leaves per species.

2.2 | A-C_i curve measurements

A-C_i curves of trees are often measured on detached branches (e.g., Bahar et al., 2017), but branch excision may lead to changes in hydraulic properties, especially in latex-producing species, where the latex clogs the xylem upon excision (Santiago & Mulkey, 2003). Lowered stomatal conductance may lead to truncated response curves, complicating parameter estimation. Because three of the four species in the current study produce latex (Table 1), we measured all parameters of interest on intact, attached leaves in situ. In the field, low leaf temperatures are rare in the afternoon, so testing the degree of hysteresis of gas-exchange parameters was not feasible. However, by measuring A-C_i curves at high temperature both before and after solar noon (Figure S1), we made sure that our results do not simply reflect diurnal patterns but indeed represent temperature responses.

Between November 2016 and February 2017, we measured A-C_i curves on sun-exposed leaves over as wide a temperature range as possible (see Table 1), making use of ambient temperature changes and controlling the block temperature of the cuvette using the Peltier cooling/heating capacity of the LI-6400 portable photosynthesis system (LI-COR Biosciences, Lincoln, Nebraska, USA). Measurements continued into the dry season, and when the soil started to dry in February, plants were watered twice a week. There were no trends in gas-exchange parameters with progression of the dry season.

Repeated measurements of the same leaf may result in stomatal closure independent of temperature or VPD, so we measured each leaf only once, thereby generating temperature-response curves not at the leaf level but at the species level (as in Slot & Winter, 2017a). Measurements were made on leaves between 0.7 and 1.7 m above the ground. Each species was measured at a range of temperatures on 5 to 8 days. The light intensity was set to a predetermined saturation level of 1,500 $\mu mol m^{-2} s^{-1}$. At high measurement temperature, the incoming air was humidified by moistening the soda lime in the column through which ambient air entered the LI-6400. Light-saturated photosynthesis rates were determined at ≥13 CO_2 concentrations between 50 and 1,800 ppm, using the built-in CO_2 mixer of the LI-6400 to control CO_2 concentrations, maintaining a flow rate of 500 $\mu mol s^{-1}$. Leaf temperature during measurement was monitored with a nickel-chromium thermocouple, attached abaxially to the leaf inside the cuvette. After equilibration at 400 ppm CO_2, photosynthesis was generally recorded at 50, 100, 200, 300, 400, 450, 500, 550, 625, 700, 900, 1,250, and 1,800 ppm CO_2 of the incoming air. At leaf temperatures >~33 °C, stomatal conductance often dropped gradually during the measurements, leading to declining rather than stabilizing photosynthesis rates during the equilibration period. When this was observed, the measurements were discontinued and a new leaf was studied, because A-C_i curves based on non-steady-state measurements do not yield reliable estimates of V_{CMax} and J_{Max}. Despite humidifying the incoming air to reduce the VPD at high leaf temperature, obtaining meaningful response curves at temperatures >35 °C was challenging. The relationship between temperature and relative humidity experienced by leaves inside the cuvette was similar to that of the ambient air to which leaves were exposed to in situ while not being measured (Figure S2), and this relationship was similar across species (Figure S3).

Concentration gradients between the leaf cuvette and the atmosphere can cause CO_2 to diffuse into or out of the cuvette, which is then erroneously assigned to the photosynthetic flux. We therefore quantified the diffusion errors by measuring CO_2-response curves for dead leaves and corrected photosynthesis and C_i values accordingly. Leaves were killed by submersion in boiling water (Flexas et al., 2007), for 2–10 min, depending on species, and CO_2-response curves were measured at 2–4 target temperatures between 26 and 36 °C. This protocol was repeated after replacing the gaskets of the leaf cuvette.

2.3 | Light respiration

Respiration in the light was estimated at different leaf temperatures according to Laisk (1977). In brief, CO_2-response curves were measured in the low CO_2 range (for most leaves, we used 45, 60, 75, 100, 125, and 200 ppm) at several different light levels (600, 200, and 100 $\mu mol m^{-2} s^{-1}$); the intersection point of the curves at different light levels indicates Γ*, the CO_2 compensation point in the absence of respiration (apart from photorespiration). R_{Light} is the CO_2 exchange rate associated with Γ*. When photosynthesis at 200 ppm CO_2 deviated from the linear part of the curve, this point was omitted to avoid introducing errors (Walker & Ort, 2015). For all leaves for which the three linear fits of diffusion-corrected net photosynthesis versus C_i intersected in one place, Γ* was calculated as

$$\Gamma^* = \frac{\text{Intercept}_{600} - \text{Intercept}_{100}}{\text{Slope}_{100} - \text{Slope}_{600}}, \quad (1)$$

where the subscripts refer to the irradiance level, and the slopes and intercepts describe the linear fits of the CO_2-response curves at those irradiance levels. From these data, species-specific relationships between Γ* and temperature and between R_{Light} and temperature were determined.

2.4 | Leaf chemical and morphological traits

For each species, three leaves were collected, leaf area was determined with an LI-3100 leaf area metre (LI-COR), and leaves were dried at 70 °C until stable mass and weighed to determine leaf mass per area (LMA). Leaf nitrogen (N) content was measured using a Thermo Flash EA1112 analyser (Waltham, MA, USA).

2.5 | Leaf temperature monitoring

To characterize the thermal environment of sun-exposed leaves of each species, we measured leaf temperatures with fine-wire copper-constantan thermocouple wires attached abaxially with Transpore™ surgical tape (3M, Maplewood, MN, USA) to 4–7 leaves per species, logging the data every minute to a CR10X datalogger (Campbell Scientific, Logan, UT, USA). Each species was monitored for ~5 days in the early dry season.

2.6 | Parameter calculation

CO_2-diffusion errors were independent of leaf temperature, but not identical across species. We therefore used species-specific, but

temperature-independent error corrections to adjust photosynthesis and C_i prior to A-C_i curve fitting (Figure 1).

V_{CMax} and J_{Max} were calculated from the corrected A-C_i curves according to the Farquhar, von Caemmerer, and Berry model (FvCB model; Farquhar, von Caemmerer, & Berry, 1980; von Caemmerer & Farquhar, 1981) with the "fitaci" function from the "plantecophys" package (Duursma, 2015) in R version 3.3.2 (R Development Core Team, 2016). The "fitaci" function uses the temperature dependencies of the CO_2 compensation point (Γ*) and the Michaelis–Menten constants of Rubisco activity for CO_2 and O_2 from Bernacchi, Singsaas, Pimentel, Portis, and Long (2001). Visual evaluation of the curves revealed no evidence for TPU limitation (see, e.g., Figure 1), and hence, TPU limitation was not considered in the calculations. At current ambient [CO_2], TPU is indeed unlikely to limit photosynthesis, given the high ambient temperatures in the lowland tropics (e.g., Sage & Kubien, 2007). The thus calculated V_{CMax} and J_{Max} values slightly underestimate the chloroplastic rates, as mesophyll conductance (G_m, the conductance for CO_2 transfer from the substomatal cavity to the site of carboxylation in the chloroplast) was assumed to be infinite. G_m can be estimated from gas exchange data alone in the absence of carbon isotope fractionation or chlorophyll fluorescence measurements, but this approach is not highly recommended because it requires a priori assignation of data points to different limitations (RuBP-carboxylation, RuBP-regeneration, TPU); the results can be challenging to interpret as estimates can be affected by changes in V_{CMax}; and it assumes that G_m is stable across a wide range of [CO_2] (Pons et al., 2009). Furthermore, the temperature response of G_m is highly species-specific (von Caemmerer & Evans, 2015), and we did not want to make assumptions about G_m that could influence the calculated temperature dependence of V_{CMax} and J_{Max}. R_{Light} was not measured on the same leaves as the A-C_i curves, but using the species-specific temperature-response curves of R_{Light}, we calculated an R_{Light} value for every measurement temperature as model input. Similarly, Γ* estimates were calculated for each temperature from the temperature-response curves of Γ* determined with the Laisk method.

2.7 | Temperature responses of V_{CMax} and J_{Max}

For the analysis of the temperature relationships of photosynthetic parameters, data collected on different trees and on different days were pooled for each species. On each measurement day, both low and high temperature measurements were made to avoid systematic bias in the temperature-response curves fitted through the pooled data.

The relationships of V_{CMax} and J_{Max} with leaf temperature in Kelvin (T_k) were fitted according to Medlyn et al. (2002) as

$$f(T_k) = k_{Opt} \times \frac{e^{\left(\frac{H_a \times (T_k - T_{Opt})}{T_k \times R \times T_{Opt}}\right)}}{H_d - H_a \times \left(1 - e^{\left(\frac{H_d \times (T_k - T_{Opt})}{T_k \times R \times T_{Opt}}\right)}\right)}, \quad (2)$$

where k_{Opt} is V_{CMax} or J_{Max} at T_{Opt} in Kelvin, H_a describes the exponential rise of the curve before T_{Opt}, equivalent to the activation energy in an Arrhenius function, H_d is the "deactivation energy," reflecting the rate of decrease above T_{Opt}, and R is the universal gas

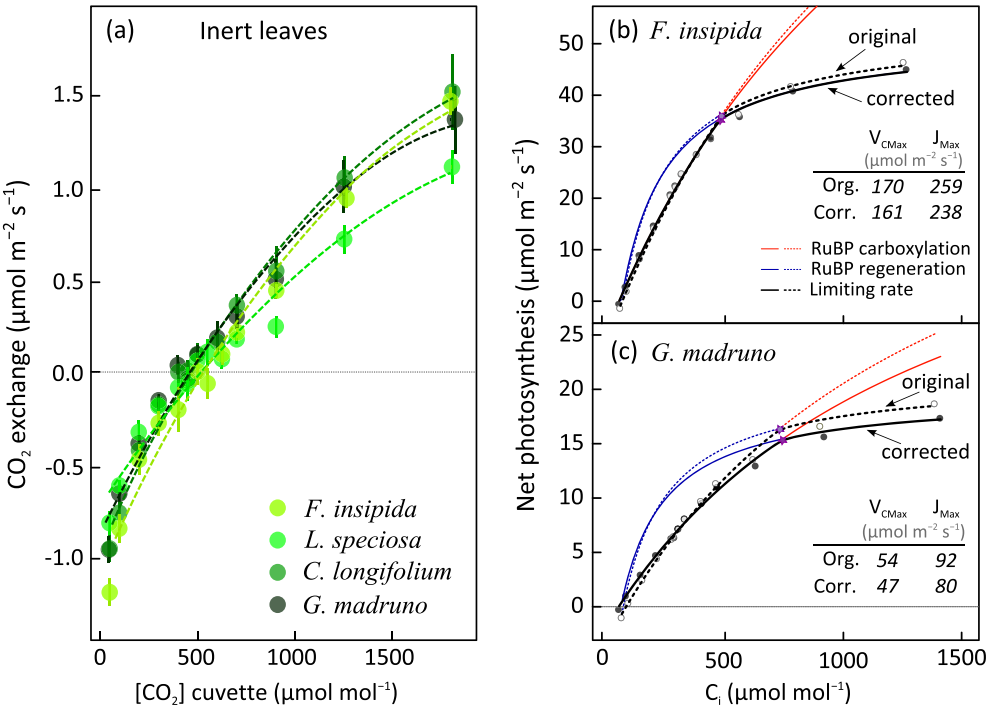

FIGURE 1 Illustration of the species-specific, [CO_2]-dependent error in photosynthesis measurements caused by CO_2 diffusion into and out of the cuvette (a), and the effects of this error for the calculation of V_{CMax} and J_{Max} in a species with high rates of photosynthesis (b, *Ficus insipida*) and a species with low rates of photosynthesis (c, *Garcinia madruno*). Photosynthesis data were corrected prior to analyses of derived parameters. *L. speciosa*: $y = -3.0 \times 10^{-7} \times ^2 + 0.0015 \times -0.717$ ($r^2 = .97$). *F. insipida*: $y = -4.6 \times 10^{-7} \times ^2 + 0.0022 \times -1.051$ ($r^2 = .97$). *C. longifolium*: $y = -4.7 \times 10^{-7} \times ^2 + 0.0022 \times -0.914$ ($r^2 = .98$). *G. madruno*: $y = -4.8 \times 10^{-7} \times ^2 + 0.0021 \times -0.862$ ($r^2 = .98$) [Colour figure can be viewed at wileyonlinelibrary.com]

constant (8.314 $JK^{-1}mol^{-1}$). In Medlyn et al. (2002) and many later publications, H_d was fixed at 200 $kJmol^{-1}$. We estimated all four parameters, including H_d but, for comparison, also fitted the curves with H_d fixed at 200 $kJmol^{-1}$. Obtaining robust parameter estimates for complex models such as Equation 2 requires more independent observations than are typically collected when remeasuring individual leaves. By combining leaves that were each measured only once, we avoided overfitting and had enough independent data points per species to estimate all parameters of the temperature response curves.

Temperature responses of all parameters were also fitted with a much simpler equation developed for J_{Max} by June, Evans, and Farquhar (2004):

$$k\,(T_k) = k_{Opt} \times e^{-\left(\frac{T_k - T_{Opt}}{\Omega}\right)^2}, \quad (3)$$

where Ω is the temperature difference between T_{Opt} and the temperature at which k is reduced to e^{-1} (~37%) of its value at T_{Opt}; it describes the "sharpness" of the peak of the symmetrical curve.

Net photosynthesis at 400 ppm (A_{400}) was extracted from each A-C_i curve, and A_{400} as a function of leaf temperature was fitted with Equation 3 to determine T_{Opt} of A_{400}. These steps were repeated for photosynthesis at 300 ppm CO_2 (A_{300}), 600 ppm (A_{600}), and at 900 ppm (A_{900}).

2.8 | Stomatal limitation

Stomatal limitation of net photosynthesis ("l") was calculated following Farquhar and Sharkey (1982) by comparing observed rates of photosynthesis with rates expected at infinite stomatal conductance:

$$l = 1 - \frac{A_{Observed}}{A_{(infinite\ G_s)}}, \quad (4)$$

where $A_{(infinite\ G_s)}$ is calculated from the FvCB model by setting C_i to equal the CO_2 concentration in the cuvette (C_a) in Equation 5:

$$V_{CMax} = \frac{A_{gross} \times (C_i + K_c)}{C_i - \Gamma^*}, \quad (5)$$

where A_{gross} equals light-saturated photosynthesis + R_{Light}, and K_c is the Michaelis–Menten constant of Rubisco activity for CO_2.

2.9 | Rubisco activase effects on photosynthesis

We assessed the effect of Rubisco activase on net photosynthesis using the method described in Sage, Way, and Kubien (2008). Declining activity of Rubisco activase at high temperature may reduce the activation state of Rubisco and thereby limit photosynthesis (Crafts-Brandner & Salvucci, 2000). However, to sustain high activity, Rubisco activase requires ample ATP supply, and if the electron transport rate (i.e., J_{Max}) is reduced at high temperature, the resulting reduction in ATP supply could inhibit Rubisco activase. To determine whether Rubisco activase limits net photosynthesis at high temperature independent of decreasing J_{Max}, we determined the effect of temperature on Rubisco activase at low [CO_2], where electron transport does not limit photosynthesis. We assessed the role of Rubisco activase by comparing measurements of the initial slopes of A-C_i curves—that is, at low [CO_2] where the ATP supply is nonlimiting to Rubisco activase—with slope estimates that were derived from a model that assumes that Rubisco is fully activated. The method thus consists of testing this model against observations, and by extension, testing the assumptions in the model. The initial slope was modelled as

$$\text{Initial slope} = \frac{V_{CMax}}{\left(\Gamma^* + K_c \times \left(1 + \frac{O}{K_o}\right)\right)}, \quad (6)$$

where K_c and K_o are the Michaelis–Menten constants of Rubisco activity for CO_2 and O_2, respectively, and O is the oxygen concentration in the chloroplast stroma. Γ* was estimated for each temperature as before, O was assumed to equal 210 mbar, and K_c and K_o were taken from Bernacchi et al. (2001). Measurements of the initial slope for each leaf—simple linear regressions—used all datapoints with C_i < 200 µmol $mol^{-1}CO_2$. When measured slopes are lower than modelled slopes, the assumption of fully activated Rubisco is invalidated and deactivation of Rubisco is implied. By plotting the initial slopes against leaf temperature, the temperature at which Rubisco activase limitation occurs can be determined.

2.10 | Statistical analyses

All nonlinear curve fitting was done with nonlinear least squares analyses using the "nls" function in the "stats" package in R. Differences in temperature-response parameters among species and between V_{CMax} and J_{Max} were determined by checking for overlap of the 95% confidence intervals. Comparisons between early successional and late-successional species were made with *t* tests. Simple linear regressions were analysed with the "lm" function in R. To identify the best predictors of net photosynthesis rate across different temperature ranges, we used the subset selection method for multiple regression (Miller, 2002) from the "Leaps" package, which identifies the best combination of predictors for any subset size from all possible combinations of those predictors, using r^2, adjusted r^2, and Mallows' C_p (Mallows, 1973) as selection criteria. To verify the implications of different thermal optima and temperature sensitivities of biochemical, stomatal, and respiratory limitations for net photosynthesis rates, we simulated net photosynthesis with the FvCB model using the "Photosyn" function from the plantecophys package (Duursma, 2015). In these simulations, we used all measured parameter values as input and compared the modelled photosynthesis rates with rates that were obtained in simulations in which V_{CMax}, J_{Max}, G_s, or R_{Light} were increased by 50%, either individually, or in combinations. All analyses were performed in R, version 3.3.2.

3 | RESULTS

A total of 149 A-C_i curves were included in the final analyses (Table 1) after 29 curves were discarded because they could not be fitted with the standard iterative method of the fitaci function, or because visual inspection indicated that they were of poor quality. Early successional species *L. speciosa* had the lowest LMA while late-successional *C. longifolium* had the highest LMA (Table 1). These species also had the smallest and largest diffusion error, respectively (Figure 1a). The

species-specific diffusion error correction that we applied to the raw data resulted in a considerable reduction of V_{CMax} from an average of 5% in *F. insipida* and *L. speciosa* to 13% in *G. madruno*. The reduction in J_{Max} ranged from 7% in *L. speciosa* to 14% in *G. madruno*. The percent reduction in process rates was inversely proportional to absolute V_{CMax} and J_{Max} values (Figure 1b). Despite these systematic changes in parameter estimates, T_{Opt} for these parameters was not affected by error correction (data not shown).

3.1 | Temperature response of biochemical parameters

3.1.1 | Maximum rate of RuBP-carboxylation, V_{CMax}

T_{Opt} of V_{CMax}, calculated with Equation 2 with four free parameters, ranged from 32.9 °C in *C. longifolium* to 39.7 °C in *L. speciosa* (Table 2). T_{Opt} was highest in *L. speciosa* but did not differ significantly among the other species (they had overlapping 95% confidence intervals; Figure 2). V_{CMax} at T_{Opt} was higher in early successional species than in late-successional species; especially *G. madruno* had much lower values than all other species (Table 2). Early successional species also had higher leaf N content than late-successional species (p = .003, t test; Table 2), but a positive correlation between leaf N content and V_{CMax} at T_{Opt} was not significant (p = .16). The activation energy (H_a) of V_{CMax} was reasonably well constrained around 75 kJmol^{-1} for three of the species, but H_a was 350 ± 303 kJmol^{-1} for *C. longifolium*. The deactivation energy, H_d, differed enormously among species, and its estimates were highly uncertain (Table 2). When fixing H_d to 200 kJmol^{-1}, T_{Opt} of V_{CMax} was moderately higher in all species (Table 2; Figure 2) while V_{CMax} at T_{Opt} tended to be lower. Fitting the symmetric curves of Equation 3 yielded fairly similar parameter estimates as the model with fixed H_d (Table 2), but Equation 3 tended to overestimate V_{CMax} above T_{Opt}.

When using an approximation of V_{CMax} (indicated as $\widehat{V}_{CMax}$) by estimating it with the one-point method (e.g., De Kauwe et al., 2016), T_{Opt} was similar to T_{Opt} of measured V_{CMax}. However, $\widehat{V}_{CMax}$ tended to be lower than V_{CMax}, and this discrepancy increased with increasing leaf temperature (Figure S4).

3.1.2 | Maximum rate of RuBP-regeneration, J_{Max}

The optimum temperature of J_{Max} was more constrained across species than that of V_{CMax}, with all values falling between 33.5 and 37.5 °C (Table 2). T_{Opt} of J_{Max} appeared lower than T_{Opt} of V_{CMax} in three of the four species, but this difference was significant only for *L. speciosa* (Figure 2). J_{Max} at T_{Opt} was highest in the early successional species and lowest in *G. madruno*. There was a marginally significant positive correlation between J_{Max} at T_{Opt} and leaf N content (p = .09, r^2 = .83). H_a and H_d of J_{Max} were not well constrained, and while H_a was higher, H_d was lower in the late-successional species compared to the early successional species. Fixing H_d to 200 kJmol^{-1} decreased both T_{Opt} of J_{Max} and J_{Max} at T_{Opt} in all species except *G. madruno* (Table 2). T_{Opt} and J_{Max} at T_{Opt} estimated with Equation 3 yielded comparable results to those estimated with Equation 2. The ratio of J_{Max} to V_{CMax} at T_{Opt} was lowest in the early successional *L. speciosa* (0.65–0.75, depending on the method used to fit the temperature-response curves) and highest in the late-successional *G. madruno* (1.12–1.15; Table 2). Because V_{CMax} is underestimated a bit more than J_{Max} when infinite G_m is assumed in the calculation (e.g., Sun et al., 2014), the J_{Max} to V_{CMax} ratio will have been slightly overestimated compared to the chloroplastic ratio.

3.1.3 | Rubisco activase

Initial slopes of measured A-C_i curves did not differ significantly from slopes that were modelled with the assumption of fully activated Rubisco. This is especially clear when comparing the smooth fitted

TABLE 2 Temperature response traits of biochemical controls over photosynthesis estimated with different models for four lowland tropical tree species

Species		V_{CMax}				J_{Max}			
		T_{Opt}	V_{CMax} (T_{Opt})	H_a	H_d	T_{Opt}	J_{Max} (T_{Opt})	H_a	H_d
		(°C)	(μmol m^{-2} s^{-1})	(kJmol^{-1})	(kJmol^{-1})	(°C)	(μmol m^{-2} s^{-1})	(kJmol^{-1})	(kJmol^{-1})
F. insipida	M_4	36.0 ± 0.6	218 ± 12	77 ± 19	1,049 ± 467	34.5 ± 0.5	214 ± 7	48 ± 15	600 ± 183
	M_3	36.3 ± 1.5	194 ± 1	121 ± 140	200	33.1 ± 1.2	202 ± 7	93 ± 110	200
	J	35.0 ± 0.8	198 ± 10			32.9 ± 0.4	213 ± 8		
L. speciosa	M_4	39.7 ± 0.3	346 ± 16	79 ± 7	2,975 ± 1,046	37.5 ± 0.6	226 ± 12	65 ± 14	610 ± 251
	M_3	40.3 ± 1.3	278 ± 1	107 ± 35	200	37.0 ± 1.2	205 ± 8	98 ± 51	200
	J	40.3 ± 2.1	275 ± 22			36.4 ± 0.8	206 ± 7		
C. longifolium	M_4	32.9 ± 1.0	159 ± 13	349 ± 303	450 ± 232	33.5 ± 0.7	155 ± 9	98 ± 70	467 ± 149
	M_3	33.5 ± 2.9	143 ± 10	108 ± 434	200	31.8 ± 1.4	141 ± 11	78 ± 332	200
	J	33.5 ± 0.6	156 ± 12			32.9 ± 0.4	155 ± 8		
G. madruno	M_4	37.1 ± 0.8	73 ± 6	69 ± 25	875 ± 1,126	35.3 ± 3.0	82 ± 2	250 ± 837	266 ± 745
	M_3	38.9 ± 2.3	73 ± 8	109 ± 93	200	35.6 ± 1.6	83 ± 2	51 ± 48	200
	J	38.6 ± 3.7	72 ± 8			35.5 ± 1.8	83 ± 2		

Note. Parameter estimates ±SEM were determined through optimization of Equation 2 allowing all four parameters to value (M_4), by setting H_d in Equation 2 to 200 kJmol^{-1} (three free parameters, M_3), or by using Equation 3 (J). Shown are the optimum temperature (T_{Opt}), the rates at optimum temperature [V_{CMax} (T_{Opt}) and J_{Max} (T_{Opt})], and for M_3 and M_4, the activation energy H_a and the deactivation energy H_d for the maximum rate of RuBP-carboxylation (V_{CMax}) and the maximum rate of RuBP-regeneration (J_{Max}).

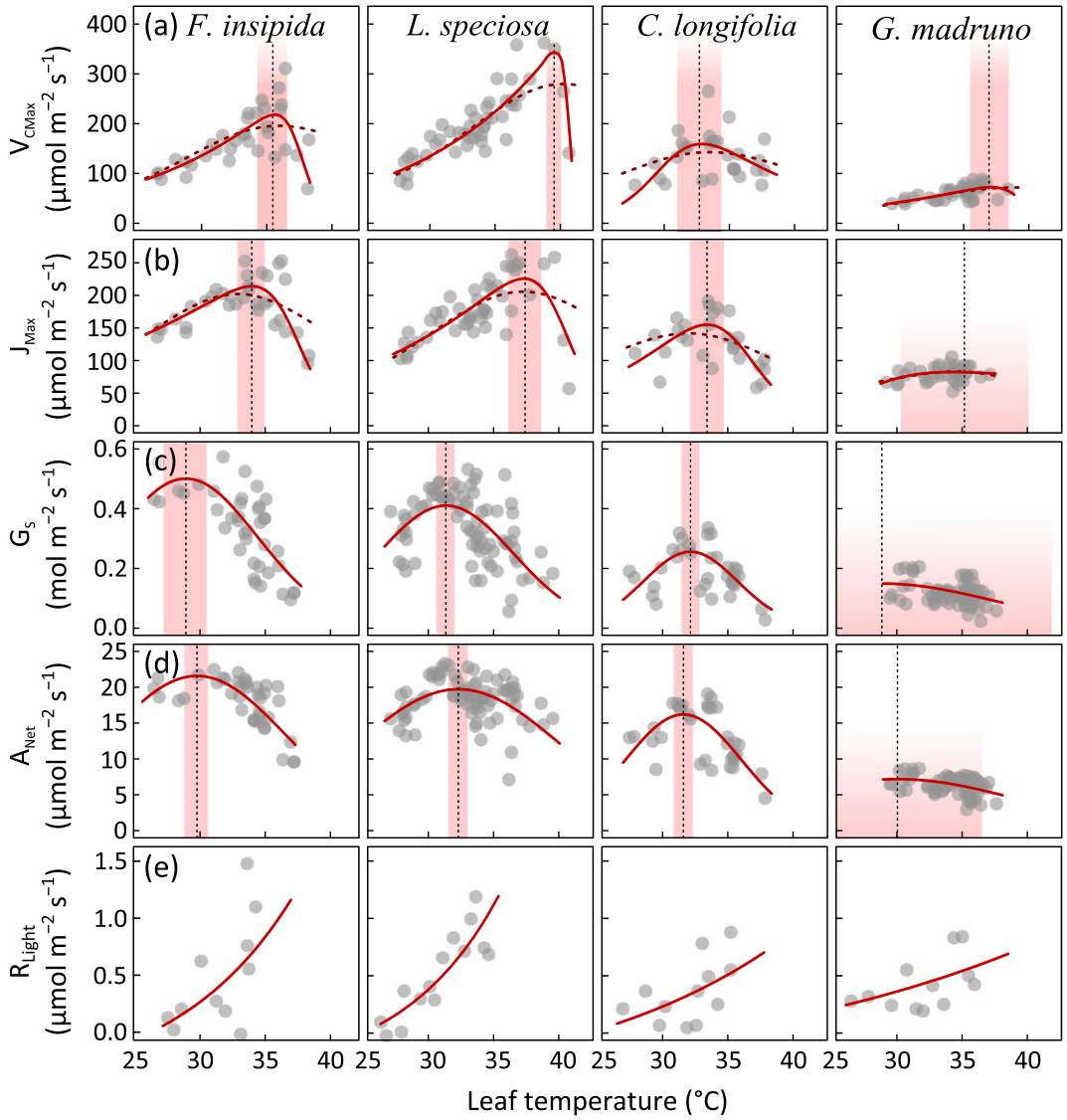

FIGURE 2 Temperature relationships of the maximum rates of RuBP-carboxylation (V_{CMax}, a) and RuBP-regeneration (J_{Max}, b), stomatal conductance (G_s, c), net photosynthesis (A_{Net}, d), and respiration in the light (R_{Light}, e) for four lowland tropical tree species. Temperature responses of V_{CMax} and J_{Max} are fitted with Equation 2 with four free parameters (solid lines) and with the deactivation energy H_d set to 200 kJmol^{-1} (dashed lines). G_s and A_{Net} are fitted with Equation 3, and for R_{Light}, exponential fits are shown. Vertical dotted lines and pink bars indicate temperature optima (T_{Opt}) calculated with Equation 4 with four free parameters and their 95% confidence intervals. T_{Opt} for V_{CMax} and J_{Max} fitted with H_d = 200 kJmol^{-1} can be found in Table 2 [Colour figure can be viewed at wileyonlinelibrary.com]

curve representing the modelled slopes in Figure 3 with the measured slopes averaged across 2 °C leaf temperature bins; even at the highest temperature, the measured values do not drop significantly below the modelled values, suggesting that over the leaf temperature, range used in the current study Rubisco-activase limitation was not a significant factor affecting net photosynthesis.

3.2 | Temperature responses of stomatal conductance and respiration in the light

T_{Opt} of stomatal conductance at 400 ppm CO_2, determined with Equation 3, was on average 30.3 ± 1.7 °C, and thus considerably lower than T_{Opt} of the biochemical parameters, except in *C. longifolium* (Figure 2). Species differed in G_s at T_{Opt}, with late-successional species *G. madruno* having average rates of 0.15 molm^{-2}s^{-1}, while early successional species *L. speciosa* and *F. insipida* had rates of 0.41 and 0.50 molm^{-2}s^{-1}, respectively. In *G. madruno* T_{Opt} was outside the measured range, and its estimate was highly uncertain (Figure 2).

R_{Light} increased with temperature in an exponential fashion (Figure 2). The rate of increase was significantly higher in the early successional than the late-successional species (p = .02; t test), but this difference did not translate into systematically higher R_{Light}: A_{Gross} ratios in early successional species at high temperatures. The R_{Light}: A_{Gross} ratio was highest for *G. madruno*, with average values ranging from 0.05 at 30 °C to 0.10 at 37 °C, compared to 0.01–0.02 at 30 °C and 0.06–0.09 at 37 °C for all other species.

3.3 | Net photosynthesis, [CO_2], stomatal limitation, and leaf temperatures

Net photosynthesis at 400 ppm CO_2 (A_{400}) peaked between 30.0 and 32.3 °C (Table 3), which roughly corresponds to the most commonly

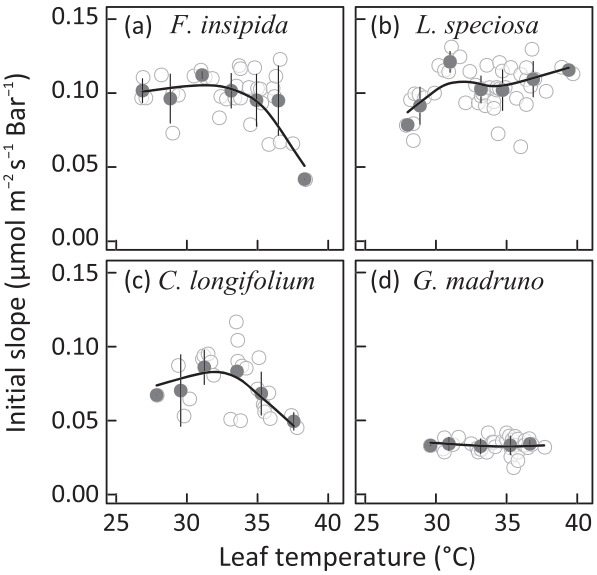

FIGURE 3 Initial slopes of A-C_i curves as a function of leaf temperature in four lowland tropical tree species. Light grey symbols are all the measured slopes, dark grey symbols are plotted as means ±SD per 2 °C leaf temperature bin; smooth solid red lines represent the modelled initial slopes calculated with Equation 6

experienced daytime leaf temperatures (Figure 4). T_{Opt} of net photosynthesis and the rate of net photosynthesis at T_{Opt} both increased with increasing measurement [CO_2], with rates more than doubling between 300 and 900 ppm CO_2, and T_{Opt} increasing by on average 2.2 °C over the same CO_2 range (Table 3; Figure 5).

As A_{400} decreased above T_{Opt}, stomatal limitation of photosynthesis significantly increased (Figure 6). *C. longifolium*, the species with the lowest temperature optima of V_{CMax} and J_{Max}, was the only species that did not display a significant increase in stomatal limitation with increasing temperature. Consistent with this, A_{400} scaled significantly with C_i: C_a ratios in all species except *C. longifolium* (slope significantly greater than zero with $p < .001$ in the early successional species and $p = .05$ in *G. madruno*), indicating that reduction in photosynthesis in all species except *C. longifolium* was associated with a draw-down of CO_2 in the substomatal cavities, and thus with increased stomatal resistance (Figure S3).

In situ leaf temperatures tended to be higher in the late-successional species, possibly as a result of their lower stomatal conductance, but because leaf temperature is strongly influenced by solar irradiance incident on the leaf surface (e.g., Rey-Sánchez, Slot, Posada, & Kitajima, 2016) and irradiance was not monitored at the leaf level, this relationship between leaf temperature and stomatal conductance could not be confirmed. Stomatal conductance and associated transpirational cooling did, however, appear to play a role in determining the frequency distribution of leaf temperatures in all species. Because the transition of leaf temperatures associated with indirect light to direct light is rapid, the frequency distributions of temperatures of sun leaves were almost bimodal (Figure 4), with the first peak—corresponding with mean daytime air temperature—associated with predominantly indirect light, near-maximum stomatal aperture, and transpirational cooling, and the second peak associated with full sun exposure, closed stomata, and minimal transpirational cooling.

3.4 | Net photosynthesis above T_{Opt}

A_{400} did not correlate significantly with V_{CMax} in the early successional species regardless of the measurement temperature range, while significant positive correlations were found for the late-successional species at almost all temperatures (Figure 7a). In all species except

TABLE 3 Temperature response traits of net photosynthesis measured at different CO_2 concentrations for four lowland tropical tree species

Species	A_{300}		A_{400}		A_{600}		A_{900}	
	T_{Opt}	A_{300} (T_{Opt})	T_{Opt}	A_{400} (T_{Opt})	T_{Opt}	A_{600} (T_{Opt})	T_{Opt}	A_{900} (T_{Opt})
	(°C)	(μmol m^{-2} s^{-1})	(°C)	(μmol m^{-2} s^{-1})	(°C)	(μmol m^{-2} s^{-1})	(°C)	(μmol m^{-2} s^{-1})
F. insipida	29.3 ± 0.7	16.1 ± 0.6	30.2 ± 0.5	21.6 ± 0.6	30.8 ± 0.6	29.0 ± 1.1	32.0 ± 0.4	34.4 ± 1.2
L. speciosa	31.4 ± 0.7	14.6 ± 0.5	32.3 ± 0.4	19.7 ± 0.4	33.2 ± 0.8	25.0 ± 1.0	34.6 ± 0.7	29.3 ± 0.9
C. longifolium	31.7 ± 0.5	11.9 ± 0.7	31.6 ± 0.4	16.2 ± 0.8	32.1 ± 0.5	22.3 ± 1.2	32.5 ± 0.4	26.3 ± 1.4
G. madruno	30.5 ± 2.5	5.4 ± 0.3	30.0 ± 3.3	7.2 ± 0.4	31.9 ± 1.2	10.6 ± 0.5	32.5 ± 0.8	13.6 ± 0.9

Note. Parameter estimates ±SEM were determined through optimization of Equation 3, the resulting curves of which are shown in Figure 5. Shown are the optimum temperature for net photosynthesis (T_{Opt}), and the rate of photosynthesis at optimum temperature for measurements at 300, 400, 600, and 900 ppm CO_2. Subscripts in the parameter names indicate the CO_2 concentration of the measurements.

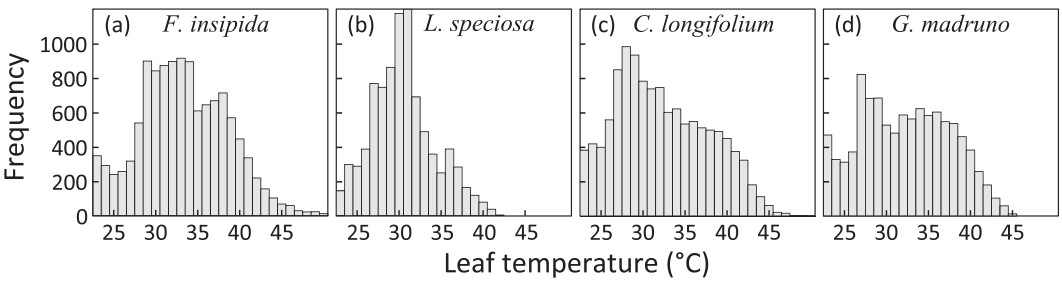

FIGURE 4 Frequency distributions of daytime (7.00–18.00) leaf temperatures of sun-exposed leaves of four tropical tree species. For each species, multiple leaves were monitored abaxially for several days, and temperatures were logged at 1–min intervals

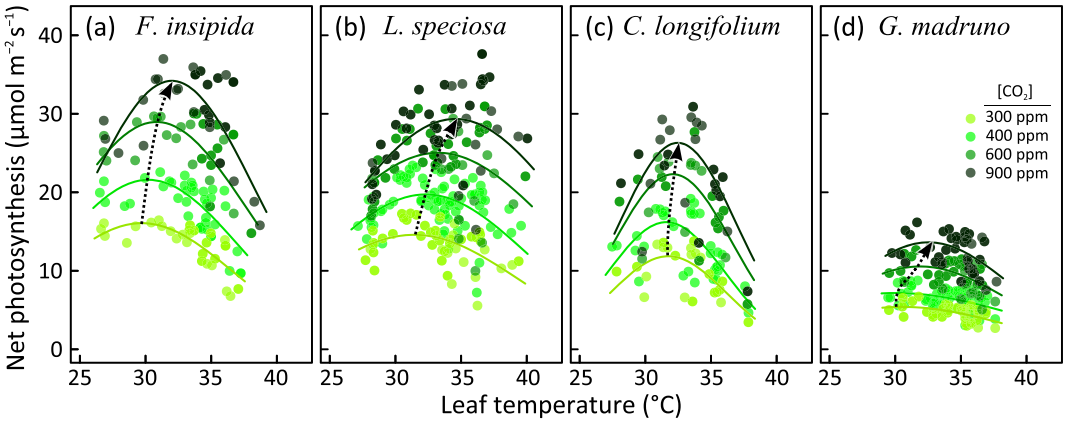

FIGURE 5 Net photosynthesis of four lowland tropical tree species as a function of leaf temperature at a range of measurement CO_2 concentrations. Curves were fitted according to Equation 3; parameter values derived from these curves can be found in Table 3. Dashed arrows indicate the shift in the maximum photosynthetic rate with increasing measurement CO_2 concentration [Colour figure can be viewed at wileyonlinelibrary.com]

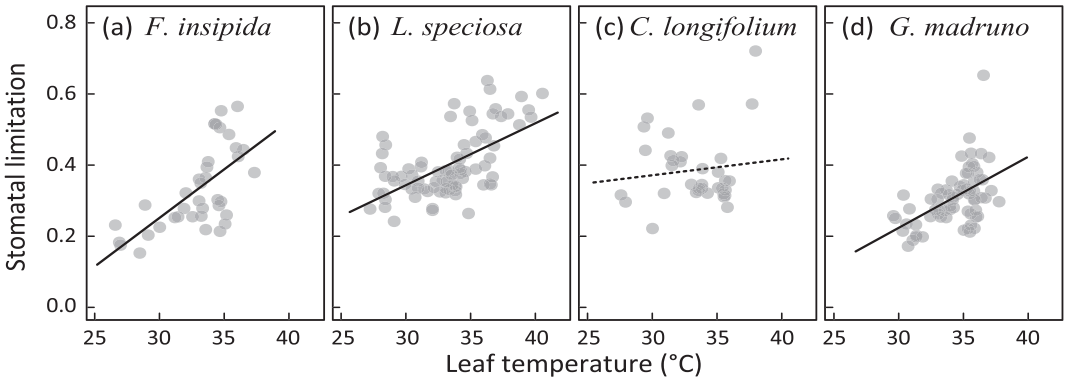

FIGURE 6 Stomatal limitation of net photosynthesis measured at 400 ppm CO_2 calculated with Equation 4 and its response to temperature in four lowland tropical tree species presented on a scale from 0—observed photosynthesis equals the hypothetical rate associated with infinite stomatal conductance—to 1—complete suppression of photosynthesis by low stomatal conductance. Solid lines indicate significant trends ($p < .01$)

C. longifolium, the steepness of the relationship increased with increasing measurement temperature range, and at higher temperatures, the relationships became marginally significant for the early successional species ($p < .1$). All species showed significant positive correlations between A_{400} and J_{Max}, and in the early successional species, the steepness of this relationship increased with increasing temperature (Figure 7b). In *L. speciosa*, this correlation was only significant >35 °C. A_{400} correlated with stomatal conductance in all species, and the strength of the correlation and the steepness of the regression slopes were mostly independent of temperature (Figure 7c). A_{400} correlated negatively with respiration in the light, and this relationship generally got steeper at higher temperatures (Figure 7d).

Stomatal conductance was the strongest single predictor for net photosynthesis when considering the full dataset, with r^2 values ranging from .44 in *G. madruno* to .78 in *C. longifolium*. As temperature approached T_{Opt} of J_{Max}, J_{Max} became the strongest predictor of net photosynthesis (Figure 8). In *C. longifolium*, J_{Max} was equally important as G_s at temperature >31 °C (r^2 = .8 for both), suggesting an earlier transition into becoming electron-transport limited than in the other species. The best two-predictor model for A_{400} always included G_s and J_{Max}.

Simulations with the FvCB model showed that increasing measured G_s by 50% stimulated modelled net photosynthesis rates, and consistent with Figure 6, this stimulation significantly increased with increasing leaf temperature (Figure S5-V). Reducing R_{Light} had a positive effect on net photosynthesis that increased significantly with increasing leaf temperature in all species, but photosynthesis was stimulated by at most ~6% (Figure S5-V). The simulations suggest that there is no overall positive correlation between leaf temperature and the stimulation of photosynthesis with an increase in J_{Max}. In fact, in *L. speciosa*, the stimulating effect that increased J_{Max} had on photosynthesis decreased with increasing temperature. However, this decrease occurred only below T_{Opt} of J_{Max}, and increasing J_{Max} above T_{Opt} did stimulate photosynthesis in all species except *G. madruno*, but with only a few datapoints above T_{Opt}, this stimulation was not always significant. In *G. madruno*—the species with the lowest V_{CMax} values and with fairly flat temperature-response curves (Figure 2)—there was a temperature-independent stimulation of photosynthesis of 25–30% with 50% increase in V_{CMax} (Figure S5-V). Increasing both G_s and J_{Max} increased the stimulation in net photosynthesis beyond that of single-parameter increase except in *G. madruno*, for which an increase in G_s and V_{CMax} had the most stimulating effect on photosynthesis of any

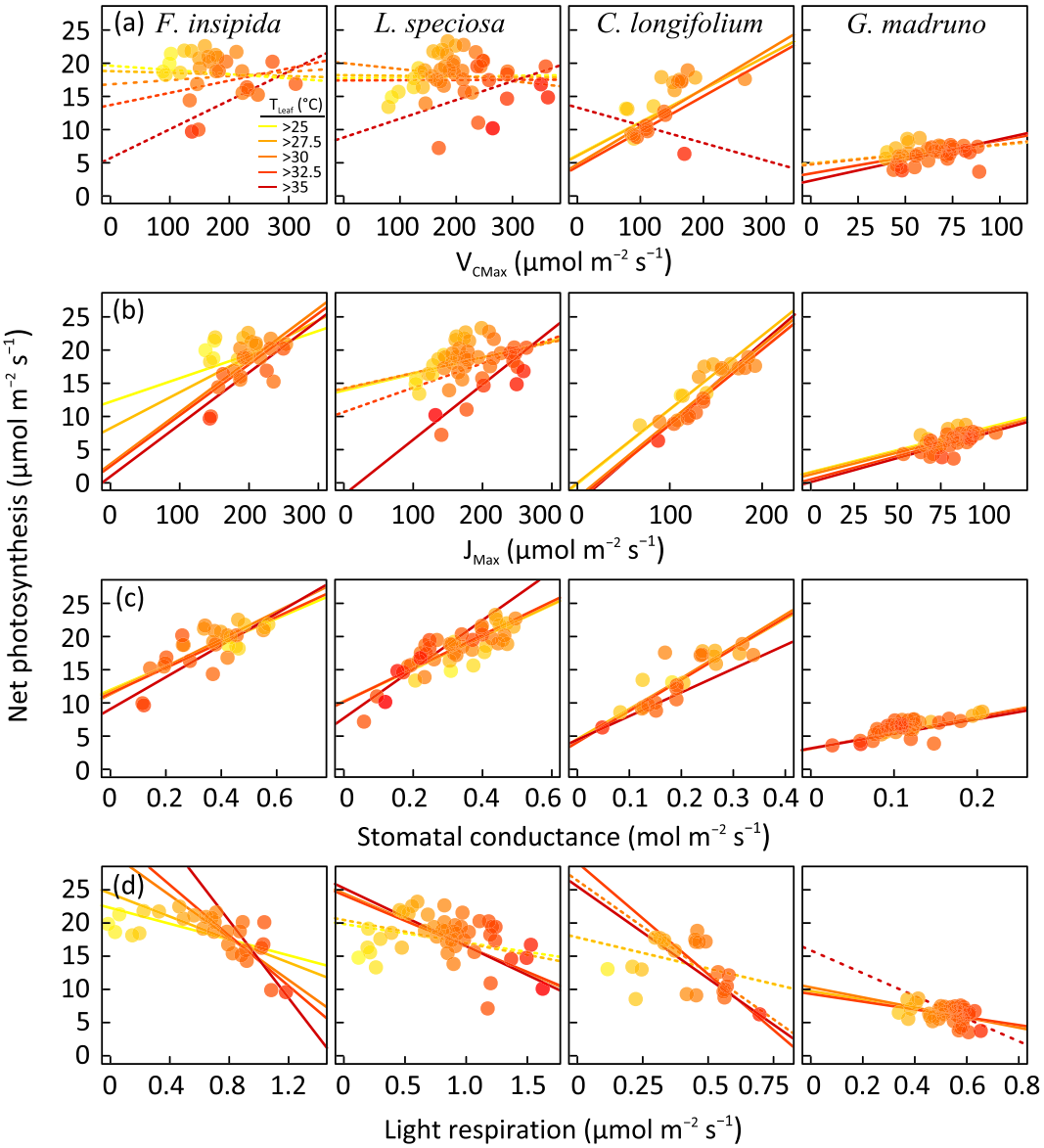

FIGURE 7 Net photosynthesis measured at 400 ppm CO_2 in relation to V_{CMax} (a), J_{Max} (b), stomatal conductance (c), and respiration in the light (d) for four lowland tropical tree species, with regression lines fitted for different measurement temperature ranges. Solid lines indicate significant fits with $p < .05$; dashed lines indicate non-significant fits [Colour figure can be viewed at wileyonlinelibrary.com]

combination (data not shown). In *C. longifolium*, in which T_{Opt} values of V_{CMax}, J_{Max}, and G_s were very similar, increasing G_s and V_{CMax} or increasing V_{CMax} and J_{Max} stimulated photosynthesis as much as increasing G_s and J_{Max}.

4 | DISCUSSION

Consistent with previous observations (Doughty & Goulden, 2008; Slot, Garcia, & Winter, 2016; Slot & Winter, 2017a), net photosynthesis of all measured species peaked near ambient daytime temperature, at about 30–32 °C, supporting our hypothesis that the optimum temperature would not differ between early successional and late-successional species. The temperature responses of underlying parameters did, however, differ considerably among species (Figure 8), but there were some general patterns. The temperature optima for RuBP-carboxylation and RuBP-regeneration were generally in the 35–40 °C range, while stomatal conductance peaked at much lower temperatures. Stomatal limitation of net photosynthesis increased with temperature and appeared to be controlling the rates of net photosynthesis for much of the measured temperature range. The increasingly strong and increasingly positive correlation between net photosynthesis and J_{Max} at high leaf temperatures suggests that photosynthesis experiences increasing limitation by photosynthetic electron transport capacity as well, although the temperature at which this happens differs among species. We found no evidence for Rubisco-activase limitation, and R_{Light} was not a major limitation to net photosynthesis at high temperatures. The inhibition of respiration by light, as inferred from the Laisk method, has recently been disputed (Farquhar & Busch, 2017), but our model simulations show that changes in R_{Light} have very minimal effects on net photosynthesis rates, so even if we underestimated R_{Light}, this is unlikely to change our conclusions. While there is uncertainty about the optimal temperatures of processes of photosynthetic biochemistry in vegetation

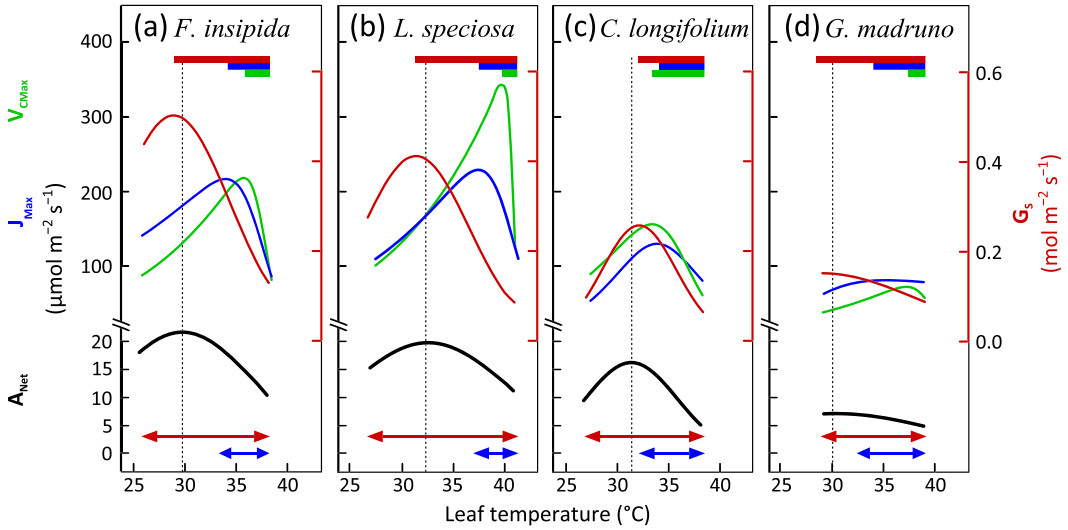

FIGURE 8 Fitted curves of maximum RuPB-carboxylation rate (V_{CMax}, green), RuBP-regeneration rate (J_{Max}, blue), stomatal conductance (G_s, red; scaled on the secondary y-axis), and net photosynthesis (A_{Net}, black) versus leaf temperature for four lowland tropical tree species. Vertical dotted lines indicate T_{Opt} of A_{Net}. Horizontal bars indicate measured temperature ranges over which V_{CMax} (green), J_{Max} (blue), and G_s (red) are decreasing. Arrows indicate the temperature ranges over which G_s (red) or J_{Max} (blue) is the strongest single predictor of A_{Net}. V_{CMax} and J_{Max} were fitted with Equation 2 (with four free parameters); A_{Net} and G_s were fitted with Equation 3 [Colour figure can be viewed at wileyonlinelibrary.com]

models (Rowland et al., 2015), our results suggest that for most of the ecologically relevant temperature range in the lowland tropics, constraining parameter estimates for stomatal conductance will be of greater importance for reducing uncertainty in simulations of biosphere–atmosphere carbon exchange in tropical forests, than constraining the optima of biochemical parameters.

4.1 | Temperature optima of biochemical parameters

We were able to identify T_{Opt} values for V_{CMax} and J_{Max} without the need to extrapolate beyond the measurement range, as has often been necessary in previous studies (e.g., Scafaro et al., 2017; some species in Vårhammar et al., 2015). Nonetheless, in *L. speciosa*, the position of T_{Opt} was driven by very few high-temperature datapoints. Our in situ approach avoided potential artefacts caused by excision of latex-producing branches (Santiago & Mulkey, 2003), or by artificial conditions of potted plants in greenhouses conditions, but it limited our ability to study leaves at very high temperature. Several previous studies were able to determine V_{CMax} and J_{Max} up to 40 °C by acclimatizing whole seedlings to elevated temperatures (e.g., Aspinwall et al., 2017; Dreyer, Le Roux, Montpied, Daudet, & Masson, 2001), while plants in the field temperatures typically close their stomata when reaching temperatures in the mid-to-high 30′s (M. Slot, personal observation). While more measurements at high temperature would improve the accuracy of the T_{Opt} estimates for *L. speciosa*, T_{Opt} of the other species was more confidently determined to be in the 33–37 °C range. These values are not substantially higher than those of cool-climate species (Kattge & Knorr, 2007; Vårhammar et al., 2015) even though Kattge and Knorr (2007) reported a positive correlation between growth temperature and T_{Opt} of V_{CMax} and J_{Max}. The temperature optima we determined fall within the range of values used in the models that Rowland et al. (2015) compared, and they fall within the observed leaf temperature range (Figure 4). Nonetheless, biochemical limitations to net photosynthesis appear to play a secondary role compared to stomatal limitation for most of the ambient temperature range.

4.2 | Stomatal conductance as key limitation of net photosynthesis

The optimum temperature was lower for stomatal conductance than for the biochemical parameters V_{CMax} and J_{Max} in three of the four species; stomatal conductance was the strongest correlate of net photosynthesis; increasing stomatal conductance above measured values in model simulations consistently stimulated net photosynthesis; this stimulation of modelled photosynthesis increased with temperature in all species, more so than stimulating other parameters did (Figure S5-V); and stomatal limitation parameter 'l' significantly increased with temperature, except in *C. longifolium*. The comparatively low optimum temperatures of J_{Max} and V_{CMax} and early onset of J_{Max} as strongest correlate of net photosynthesis in *C. longifolium* suggest a greater degree of colimitation of photosynthesis by stomatal conductance and biochemical parameters at high temperature in this species.

Strong declines in stomatal conductance above T_{Opt} in previous in situ measurements of tropical trees suggested that stomatal conductance is the major limiting factor of net photosynthesis at supra-optimal temperatures (Slot & Winter, 2017a). The current analysis confirms that the decrease in photosynthesis above T_{Opt} is primarily driven by the indirect effect of temperature—through VPD and stomatal conductance—not by the direct effect of temperature on photosynthetic biochemistry or respiratory metabolism. This is further illustrated by the similarity in the curves of photosynthesis versus leaf temperature and photosynthesis versus VPD, a similarity that is driven by the strong effect of leaf temperature on VPD (Figures S3 and S6). At higher temperatures, electron transport rates do decrease (Figure 8; Wise, Olson, Schrader, & Sharkey, 2004; Sage & Kubien, 2007; Vårhammar et al., 2015), but the effect of this on net photosynthesis for field-grown tropical forest trees is probably small. A-C_i-based

studies systematically underestimate the importance of stomatal closure for photosynthesis at high temperature, because of the inherent selection bias favouring leaves with open stomata to obtain meaningful A-C_i curves. In most leaves of the trees studied here, including *C. longifolium*, stomata closed at temperatures in the mid-to-high 30 °C's. If these leaves would be taken into consideration, an even stronger stomatal limitation would be inferred. Even among the measured leaves, stomatal conductance had already decreased by 30–50% relative to its maximum when temperatures reach T_{Opt} of J_{Max}, so it is likely that even at supra-optimal temperatures for J_{Max}, CO_2 reaching the chloroplasts is a much stronger limitation than electron transport rate. The fact that by the time leaves in the field reach temperatures supra-optimal for J_{Max}, the stomata typically are fully closed renders potential electron transport limitations largely irrelevant under field conditions. Our results for tropical trees, based on a thorough study of attached leaves in situ, are consistent with model simulations at the leaf and biome level (Lloyd & Farquhar, 2008; Rowland et al., 2015) and with observations at the stand level (Tan et al., 2017; Wu et al., 2017).

Although net photosynthesis of these tropical trees is clearly limited by stomatal conductance at high temperatures, mesophyll conductance (G_m) may also impose a significant limitation. However, despite progress in our mechanistic understanding of G_m and its regulation (e.g., von Caemmerer & Evans, 2015; Qui et al. 2017; Xiao & Zhu, 2017), the temperature response of G_m remains poorly resolved and appears to be highly species-specific (Flexas, Ribas-Carbó, Diaz-Espejo, Galmés, & Medrano, 2008; von Caemmerer & Evans, 2015). Furthermore, most Earth system models do not yet include G_m (Rogers et al., 2017; Sun et al., 2014). Generally, G_m either increases and then plateaus at high temperature, or it starts decreasing above 30 to 35 °C (reviewed in Flexas et al., 2008 and Qiu et al., 2017). Data for tropical forest plants are rare. G_m of the one tropical tree species in von Caemmerer and Evans (2015) peaked at ~35 °C, while Pons and Welschen (2003) showed a marginal decline in G_m between 28 and 38 °C for *Eperua grandiflora*, another tropical tree species. Clearly, more measurements would be required to establish the contribution of G_m to the decline in net photosynthesis above current ambient temperatures in tropical forest species.

4.3 | Species differences and sampling challenges in hyper-diverse tropical forests

The highest temperature optima for V_{CMax} and J_{Max} were found in *L. speciosa*, a species native to south Asia, where maximum temperatures are higher than in Panama. The lowest optima were found in *C. longifolium*, a Neotropical late-successional species. Interestingly, T_{Opt} of net photosynthesis was almost identical for these two species (Table 3). Although well-replicated at the leaf-level, species in the current study were not represented by many individuals. Nonetheless, the apparent species differences in the regulation of temperature responses of photosynthesis are disconcerting given the species richness of tropical forests and the desire for a simple, mechanistic understanding of how tropical species at large behave at high temperature, for the sake of modelling climate change effects on tropical vegetation. While some species differences were consistent with species' functional groups (e.g., greater temperature sensitivity of R_{Light}, and lower activation energy of V_{CMax} in early successional species than in late-successional species), others were not. Identifying commonality in control processes will be instrumental for reducing the uncertainty of ecosystem models, but determining biochemical parameters and R_{Light} is labour-intensive, and tropical species richness is high. We assessed the utility of estimating V_{CMax} with the one-point method when studying temperature relations (Figure S4), and while we have greater confidence in the absolute values of V_{CMax} determined from A-C_i curves than in estimates derived from the one-point method (see Figure S4), the one-point method is very rapid. When assessing the effects of high temperature, progressive stomatal closure during A-C_i curve measurements may compromise the quality of the curves. Measurements after quick equilibration at ambient CO_2, or even rapid nonequilibration A-C_i measurements (Stinziano et al., 2017), may increase the chances of obtaining useful high temperature data and enable the assessment of a larger number of species and individuals per species.

4.4 | Concluding remarks and outlook

Net photosynthesis of lowland tropical trees peaks close to ambient daytime temperature, despite some species differences in the temperature responses of the factors controlling net photosynthesis. The indirect effect of temperature—through VPD and stomatal conductance—is consistently a stronger limitation of net photosynthesis than the direct effect of temperature on biochemical process rates, especially when considering that many leaves with very low stomatal conductance were excluded from A-C_i curve measurements. These results stress the importance of parameterizing stomatal properties in relation to temperature, VPD, and soil hydraulic conditions to better simulate the carbon dynamics of tropical forest trees in the face of atmospheric and climate change. And although challenging experimentally, disentangling temperature effects from VPD effects on stomatal conductance will be particularly valuable for understanding and modelling photosynthesis in a changing climate (Peak & Mott, 2011).

As temperature continues to rise, thermal acclimation will likely increase the optimum temperature of photosynthesis (Slot & Winter, 2017b). Rising atmospheric [CO_2] will further increase the temperature optimum by lowering photorespiration (Figure 5; Cernusak et al., 2013). On the other hand, lower stomatal conductance associated with elevated CO_2 may reduce transpirational cooling and increase leaf temperatures. At higher [CO_2], TPU may also become limiting (Sage & Kubien, 2007), particularly because low phosphorus availability in tropical forests (e.g., Vitousek, Porder, Houlton, & Chadwick, 2010) may enhance TPU limitation (Ellsworth, Crous, Lambers, & Cooke, 2015). Given that differences in thermal optima of biochemical control factors of photosynthesis exist among species, an important challenge will be to describe the long-term effects of climate change in terms of changes in the stomatal and biochemical properties of tropical tree species, and to identify general patterns across species to facilitate predictions of long-term changes across the tropics.

ACKNOWLEDGMENTS

This research was supported by the Smithsonian Tropical Research Institute (STRI). MS was recipient of an Earl S. Tupper–STRI postdoctoral fellowship.

ORCID

Martijn Slot http://orcid.org/0000-0002-5558-1792

REFERENCES

Ahlström, A., Schurgers, G., Arneth, A., & Smith, B. (2012). Robustness and uncertainty in terrestrial ecosystem carbon response to CMIP5 climate change projections. *Environmental Research Letters*, *7*. 044008.

Aspinwall, M., Vårhammar, A., Blackman, C., Tjoelker, M., Ahrens, C., Byrne, M., … Rymer, P. (2017). Adaptation and acclimation both influence photosynthetic and respiratory temperature responses in *Corymbia calophylla*. *Tree Physiology*, *37*, 8, 1095–1112.

Bahar, N. H., Ishida, F. Y., Weerasinghe, L. K., Guerrieri, R., O'Sullivan, O. S., Bloomfield, K. J., … Atkin, O. K. (2017). Leaf-level photosynthetic capacity in lowland Amazonian and high-elevation Andean tropical moist forests of Peru. *New Phytologist*, *214*, 1002–1018.

Bernacchi, C. J., Singsaas, E. L., Pimentel, C., Portis, A. R. Jr., & Long, S. P. (2001). Improved temperature response functions for models of Rubisco-limited photosynthesis. *Plant, Cell and Environment*, *24*, 253–259.

Brooks, A., & Farquhar, G. D. (1985). Effect of temperature on the CO_2/O_2 specificity of ribulose-1,5-bisphosphate carboxylase oxygenase and the rate of respiration in the light—Estimates from gas-exchange measurements on spinach. *Planta*, *165*, 397–406.

Cernusak, L. A., Winter, K., Dalling, J. W., Holtum, J. A., Jaramillo, C., Körner, C., … Wright, S. J. (2013). Tropical forest responses to increasing atmospheric CO2: Current knowledge and opportunities for future research. *Functional Plant Biology*, *40*, 531–551.

Cox, P. M., Pearson, D., Booth, B. B., Friedlingstein, P., Huntingford, C., Jones, C. D., & Luke, C. M. (2013). Sensitivity of tropical carbon to climate change constrained by carbon dioxide variability. *Nature*, *494*, 341–344.

Crafts-Brandner, S. J., & Salvucci, M. E. (2000). Rubisco activase constrains the photosynthetic potential of leaves at high temperature and CO_2. *Proceedings of the National Academy of Sciences*, *97*, 13430–13435.

De Kauwe, M. G., Lin, Y. S., Wright, I. J., Medlyn, B. E., Crous, K. Y., Ellsworth, D. S., … Domingues, D. T. (2016). A test of the 'one-point method' for estimating maximum carboxylation capacity from field-measured, light-saturated photosynthesis. *New Phytologist*, *210*, 1130–1144.

Doughty, C. E., & Goulden, M. L. (2008). Are tropical forests near a high temperature threshold? *Journal of Geophysical Research – Biogeosciences*, *113*. G00B07.

Dreyer, E., Le Roux, X., Montpied, P., Daudet, F. A., & Masson, F. (2001). Temperature response of leaf photosynthetic capacity in seedlings from seven temperate tree species. *Tree Physiology*, *21*, 223–232.

Duursma, R. A. (2015). Plantecophys-an R Package for analysing and modelling leaf gas exchange data. *PLoS One*, *10*. e0143346.

Ellsworth, D. S., Crous, K. Y., Lambers, H., & Cooke, J. (2015). Phosphorus recycling in photorespiration maintains high photosynthetic capacity in woody species. *Plant, Cell and Environment*, *38*, 1142–1156.

Farquhar, G. D., & Busch, F. A. (2017). Changes in the chloroplastic CO_2 concentration explain much of the observed Kok effect: A model. *New Phytologist*, *214*, 570–584.

Farquhar, G. D., & Sharkey, T. D. (1982). Stomatal conductance and photosynthesis. *Annual Review of Plant Physiology*, *33*, 317–345.

Farquhar, G. D., von Caemmerer, S., & Berry, J. A. (1980). A biochemical model of photosynthetic CO_2 assimilation in leaves of C3 species. *Planta*, *149*, 78–90.

Flexas, J., Díaz-Espejo, A., Berry, J. A., Cifre, J., Galmés, J., Kaldenhoff, R., … Ribas-Carbó, M. (2007). Analysis of leakage in IRGA's leaf chambers of open gas exchange systems, quantification and its effects in photosynthesis parameterization. *Journal of Experimental Botany*, *58*, 1533–1543.

Flexas, J., Ribas-Carbó, M., Diaz-Espejo, A., Galmés, J., & Medrano, H. (2008). Mesophyll conductance to CO_2: Current knowledge and future prospects. *Plant, Cell and Environment*, *31*, 602–621.

Huntingford, C., Zelazowski, P., Galbraith, D., Mercado, L. M., Sitch, S., Fisher, R., … Cox, P. M. (2013). Simulated resilience of tropical rainforests to CO_2-induced climate change. *Nature Geoscience*, *6*, 268–273.

June, T., Evans, J. R., & Farquhar, G. D. (2004). A simple new equation for the reversible temperature dependence of photosynthetic electron transport: A study on soybean leaf. *Functional Plant Biology*, *31*, 275–283.

Kattge, J., & Knorr, W. (2007). Temperature acclimation in a biochemical model of photosynthesis: A reanalysis of data from 36 species. *Plant, Cell and Environment*, *30*, 1176–1190.

Laisk, A. (1977). *Kinetics of photosynthesis and photorespiration in C3 plants [In Russian]*. Moscow: Nauka.

Lin, Y. S., Medlyn, B. E., & Ellsworth, D. S. (2012). Temperature responses of leaf net photosynthesis: The role of component processes. *Tree Physiology*, *32*, 219–231.

Lloyd, J., & Farquhar, G. D. (2008). Effects of rising temperatures and $[CO_2]$ on the physiology of tropical forest trees. *Philosophical Transaction of the Royal Society B*, *363*, 1811–1817.

Mallows, C. L. (1973). Some comments on Cp. *Technometrics*, *15*, 661–675.

Medlyn, B. E., Dreyer, E., Ellsworth, D., Forstreuter, M., Harley, P. C., Kirschbaum, M. U. F., … Loustau, D. (2002). Temperature response of parameters of a biochemically based model of photosynthesis. II. A review of experimental data. *Plant, Cell and Environment*, *25*, 1167–1179.

Medvigy, D., Wofsy, S. C., Munger, J. W., Hollinger, D. Y., & Moorcroft, P. R. (2009). Mechanistic scaling of ecosystem function and dynamics in space and time: Ecosystem Demography model version 2. *Journal of Geophysical Research – Biogeosciences*, *114*. G01002.

Miller, A. (2002). *Subset selection in regression*. New York, NY, USA: Chapman & Hall.

Norby, R., Gu, L., Haworth, I., Jensen, A. M., Turner, B., Walker, A., … Winter, K. (2017). Informing models through empirical relationships between foliar phosphorus, nitrogen and photosynthesis across diverse woody species in tropical forests of Panama. *New Phytologist*, *215*, 1425–1437.

Pan, Y., Birdsey, R. A., Fang, J., Houghton, R., Kauppi, P. E., Kurz, W. A., … Hayes, D. (2011). A large and persistent carbon sink in the world's forests. *Science*, *333*, 988–993.

Pan, Y., Birdsey, R. A., Phillips, O. L., & Jackson, R. B. (2013). The structure, distribution, and biomass of the world's forests. *Annual Review of Ecology, Evolution, and Systematics*, *44*, 593–622.

Peak, D., & Mott, K. A. (2011). A new, vapour-phase mechanism for stomatal responses to humidity and temperature. *Plant, Cell and Environment*, *34*, 162–178.

Pons, T. L., Flexas, J., von Caemmerer, S., Evans, J. R., Genty, B., Ribas-Carbo, M., & Brugnoli, E. (2009). Estimating mesophyll conductance to CO_2: Methodology, potential errors, and recommendations. *Journal of Experimental Botany*, *60*, 2217–2234.

Pons, T. L., & Welschen, R. A. (2003). Midday depression of net photosynthesis in the tropical rainforest tree *Eperua grandiflora*: contributions of stomatal and internal conductances, respiration and Rubisco functioning. *Tree Physiology*, *23*, 937–947.

Qiu, C., Ethier, G., Pepin, S., Dubé, P., Desjardins, Y., & Gosselin, A. (2017). Persistent negative temperature response of mesophyll conductance in red raspberry (*Rubus idaeus* L.) leaves under both high and low vapour

pressure deficits: A role for abscisic acid? *Plant, Cell and Environment*, *40*, 1940–1959.

R Development Core Team. (2016) R: A language and environment for statistical computing. R v.3.3.2. R Foundation for Statistical Computing, Vienna, Austria.

Rey-Sánchez, C., Slot, M., Posada, J. M., & Kitajima, K. (2016). Spatial and seasonal variation of leaf temperature within the canopy of a tropical forest. *Climate Research*, *71*, 75–89.

Rogers, A., Medlyn, B. E., Dukes, J. S., Bonan, G., Caemmerer, S., Dietze, M. C., … Zaehle, S. (2017). A roadmap for improving the representation of photosynthesis in Earth system models. *New Phytologist*, *213*, 22–42.

Rowland, L., Harper, A., Christoffersen, B. O., Galbraith, D. R., Imbuzeiro, H. M. A., Powell, T. L., … Williams, M. (2015). Modelling climate change responses in tropical forests: Similar productivity estimates across five models, but different mechanisms and responses. *Geoscientific Model Development*, *8*, 1097–1110.

Sage, R. F., & Kubien, D. S. (2007). The temperature response of C3 and C4 photosynthesis. *Plant, Cell and Environment*, *30*, 1086–1106.

Sage, R. F., Way, D. A., & Kubien, D. S. (2008). Rubisco, Rubisco activase, and global climate change. *Journal of Experimental Botany*, *59*, 1581–1595.

Santiago, L. S., & Mulkey, S. S. (2003). A test of gas exchange measurements on excised canopy branches of ten tropical tree species. *Photosynthetica*, *41*, 343–347.

Scafaro, A. P., Xiang, S., Long, B. M., Bahar, N. H., Weerasinghe, L. K., Creek, D., … Atkin, O. K. (2017). Strong thermal acclimation of photosynthesis in tropical and temperate wet-forest tree species: the importance of altered Rubisco content. *Global Change Biology*, *23*, 2783–2800.

Schimel, D., Stephens, B. B., & Fisher, J. B. (2015). Effect of increasing CO_2 on the terrestrial carbon cycle. *Proceedings of the National Academy of Sciences, USA*, *112*, 436–441.

Slot, M., Garcia, M. N., & Winter, K. (2016). Temperature response of CO_2 exchange in three tropical tree species. *Functional Plant Biology*, *43*, 468–478.

Slot, M., Rey-Sánchez, C., Winter, K., & Kitajima, K. (2014). Trait-based scaling of temperature-dependent foliar respiration in a species-rich tropical forest canopy. *Functional Ecology*, *28*, 1074–1086.

Slot, M., & Winter, K. (2017a). *In situ* temperature response of photosynthesis of 42 tree and liana species in the canopy of two Panamanian lowland tropical forests with contrasting rainfall regimes. *New Phytologist*, *214*, 1103–1117.

Slot, M., & Winter, K. (2017b). Photosynthetic acclimation to warming in tropical forest tree seedlings. *Journal of Experimental Botany*, *68*, 2275–2284.

Slot, M., Wright, S. J., & Kitajima, K. (2013). Foliar respiration and its temperature sensitivity of trees and lianas: *In situ* measurements in the upper canopy of a tropical forest. *Tree Physiology*, *33*, 505–515.

Stinziano, J. R., Morgan, P. B., Lynch, D. J., Saathoff, A. J., McDermitt, D. K., & Hanson, D. T. (2017). The rapid A–Ci response: Photosynthesis in the phenomic era. *Plant, Cell and Environment*, *40*, 1256–1262.

Sun, Y., Gu, L., Dickinson, R. E., Pallardy, S. G., Baker, J., & Cao, …, Jensen A. M. (2014). Asymmetrical effects of mesophyll conductance on fundamental photosynthetic parameters and their relationships estimated from leaf gas exchange measurements. *Plant, Cell and Environment*, *37*, 978–994.

Tan, Z.-H., Zeng, J., Zhang, Y.-J., Slot, M., Gamo, M., Hirano, T., … Restrepo-Coupe, N. (2017). Optimum air temperature for tropical forest photosynthesis: Mechanisms involved and implications for climate warming. *Environmental Research Letters*, *12*, 5.

Vårhammar, A., Wallin, G., McLean, C. M., Dusenge, M. E., Medlyn, B. E., Hasper, T. B., … Uddling, J. (2015). Photosynthetic temperature responses of tree species in Rwanda: evidence of pronounced negative effects of high temperature in montane rainforest climax species. *New Phytologist*, *206*, 1000–1012.

Vitousek, P. M., Porder, S., Houlton, B. Z., & Chadwick, O. A. (2010). Terrestrial phosphorus limitation: Mechanisms, implications, and nitrogen–phosphorus interactions. *Ecological Applications*, *20*, 5–15.

von Caemmerer, S., & Evans, J. R. (2015). Temperature responses of mesophyll conductance differ greatly between species. *Plant, Cell and Environment*, *38*, 629–637.

von Caemmerer, S., & Farquhar, G. D. (1981). Some relationships between the biochemistry of photosynthesis and the gas exchange of leaves. *Planta*, *153*, 376–387.

Walker, B. J., & Ort, D. R. (2015). Improved method for measuring the apparent CO_2 photocompensation point resolves the impact of multiple internal conductances to CO_2 to net gas exchange. *Plant, Cell and Environment*, *38*, 2462–2474.

Way, D. A., Oren, R., & Kroner, Y. (2015). The space-time continuum: The effects of elevated CO_2 and temperature on trees and the importance of scaling. *Plant, Cell and Environment*, *38*, 991–1007.

Way, D. A., & Yamori, W. (2014). Thermal acclimation of photosynthesis: on the importance of adjusting our definitions and accounting for thermal acclimation of respiration. *Photosynthesis Research*, *119*, 89–100.

Williams, M. (1996). A three-dimensional model of forest development and competition. *Ecological Modelling*, *89*, 73–98.

Wise, R. R., Olson, A. J., Schrader, S. M., & Sharkey, T. D. (2004). Electron transport is the functional limitation of photosynthesis in field-grown pima cotton plants at high temperature. *Plant, Cell and Environment*, *27*, 717–724.

Wu, J., Guan, K., Hayek, M., Restrepo-Coupe, N., Wiedemann, K. T., Xu, X., … Saleska, S. R. (2017). Partitioning controls on Amazon forest photosynthesis between environmental and biotic factors at hourly to interannual timescales. *Global Change Biology*, *23*, 1240–1257.

Xiao, Y., & Zhu, X. G. (2017). Components of mesophyll resistance and their environmental responses a theoretical modeling analysis. *Plant, Cell and Environment*. In press. https://doi.org/10.1111/pce.13040

SUPPORTING INFORMATION

Additional Supporting Information may be found online in the supporting information tab for this article.

How to cite this article: Slot M, Winter K. In situ temperature relationships of biochemical and stomatal controls of photosynthesis in four lowland tropical tree species. *Plant Cell Environ*. 2017;1–14. https://doi.org/10.1111/pce.13071